^{35}Cl NQR study of the structural order-disorder transition in $(CH_3NH_3)_2MnCl_4$†

R. Kind and J. Roos

Laboratory of Solid State Physics, Swiss Federal Institute of Technology, Eidgenössische Technische Hochschule, CH-8049 Zürich, Switzerland

(Received 28 May 1975)

The temperature dependence of the ^{35}Cl nuclear quadrupole resonance (NQR) for the two chemically inequivalent chlorine sites in the perovskitic layer-structure compound $(CH_3NH_3)_2MnCl_4$ has been measured around the second-order phase transition at 393.7 K. A value of the critical exponent β of the order parameter was determined to be $\beta = 0.250 \pm 0.005$, which is intermediate between the corresponding values for the three- and the two-dimensional Ising model. A microscopic model of the phase transition is proposed, involving an order-disorder transition of the CH_3NH_3 groups. Above T_c these groups move on a conical surface between four equivalent potential wells which become inequivalent below T_c. The mechanism of this phase transition has been computer simulated in a point-charge model from which a quadratic dependence of the ^{35}Cl NQR frequencies on the order parameter is derived. Quantitative agreement between theory and experimental data is obtained by choosing appropriate values for the lattice parameters and by defining how the probability amplitudes for the four potential wells vary with the order parameter.

I. INTRODUCTION

The compound $(CH_3NH_3)_2MnCl_4$ crystalizes in a perovskite-type layer structure exhibiting several interesting structural phase transitions in the paramagnetic phase.[1] The space group in the orthorhombic room-temperature phase is *Cmca*, D_{2h}^{18}.[2] At present the atomic positions are published only for the isotype compound $(CH_3CH_2CH_2NH_3)_2MnCl_4$.[3] The structure consists of infinite sheets of $MnCl_6$ octahedra sharing corners. Such an arrangement closely resembles a plane of the perovskite structure, with Mn occupying the *B* sites (Fig. 1). There are two chemically inequivalent chlorine sites, the bonding $Cl_{(1)}$ sites in the manganese plane and the nonbonding $Cl_{(2)}$ sites above and below the manganese plane. The *A* sites in the cavities between the octahedra are occupied by the NH_3 groups of the methylammonium with an averaged C-N direction perpendicular to the plane and pointing to next $MnCl_6$ octahedra in adjacent planes. Interlayer bonding is achieved only by van der Waals forces acting between the CH_3 groups. On raising the temperature the crystal undergoes a second-order phase transition at 393.7 K leading to the tetragonal space group $I4/mmm$, D_{4h}^{17}.[2,4] For symmetry reasons this transition must be related to an order-disorder transition (change in the asymmetry of the motion) of the CH_3NH_3 groups.

Because of the analogy of the crystal structure with smectic liquid crystals and membrane structures, the motion of these CH_3NH_3 groups is of great interest. Among all the perovskite-type layer structures of the type $(C_nH_{2n+1}NH_3)_2MCl_4$ ($n = 1, \ldots, 10$, M = Mn, Fe, Cu) for which the tetragonal high-temperature phase can be reached before decomposition only two ($n = 1$, M = Mn, Fe) show a second-order phase transition.[5] With increasing n the transition temperature moves to higher values and at the same time the number of structural phase transitions occurring between room temperature and this highest transition temperature before decomposition is increased. This is certainly due to the increasing degree of freedom in the alkyl groups. In order to learn something about the nature of the complex motion of the alkyl groups we directed our nuclear-quadrupole-resonance (NQR) studies to the simplest system $(CH_3NH_3)_2MnCl_4$, and to the mechanism of the second-order phase transition at 393.7 K.

In Sec. II the NQR measurements are presented.

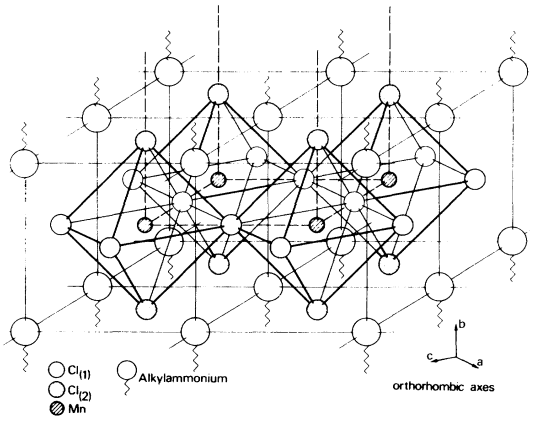

FIG. 1. Schematic representation of perovskite-type layer in $(C_nH_{2n+1}NH_3)_2MnCl_4$.

It is shown how the two observed resonance lines were identified and assigned to the two chemically inequivalent lattice sites of the chlorine nuclei. From the temperature dependence of one of the two lines a critical exponent is determined. In Sec. III a microscopic model of the phase transition is presented which is based on all experimental data known up to now. Section IV is devoted to a comparison of the NQR results with model calculations based on our microscopic model. It is divided into three parts: In the first part the electric-field-gradient (efg) tensors of the two chlorine sites are calculated for the tetragonal phase. In the second part an analytical calculation of the NQR line shift due to the phase transition is performed for the $Cl_{(2)}$ site by using a two-dimensional model. A numerical calculation with a three-dimensional point-charge model and the comparison with the experimental data are given in the last part. In Sec. V the results are summarized and discussed.

II. NQR MEASUREMENTS

Since measurements of the quadrupole coupling constants are known to be a sensitive tool for the study of structural phase transitions, we started by looking for the pure nuclear quadrupole resonances (NQR) of ^{35}Cl at room temperature with a self-quenched super-regenerative detector. The resonance condition for the strong electron-spin transition of Mn^{++} was fulfilled periodically by the magnetic field modulation over the whole scanned frequency range (3–30 MHz). This caused a strong frequency-dependent offset voltage at the lock-in detector, which hindered the measurements considerably. Two resonance lines of ^{35}Cl were found at 7.711 and 4.564 MHz corresponding to the two chemically inequivalent lattice sites of the chlorine atoms. The signals were identified by comparing the frequencies and amplitudes with those of the corresponding signals of ^{37}Cl. As in the case of the $ABCl_3$ perovskite family the ^{35}Cl NQR frequencies are rather low (e.g., in $CsPbCl_3$ $\nu_Q \sim 7.7$ MHz,[6] in $RbCdCl_3$ $\nu_Q \sim 11.2$ MHz [7]) compared with known transition frequencies in most solids.

The temperature dependence of the two ^{35}Cl transition frequencies has been measured with a Bruker NMR pulse spectrometer in the phase-sensitive mode. The lock-in frequency was adjusted well above or below the resonance frequency in order to obtain an undistorted line shape from the Fourier transform of the signal decay. The signals were extremely weak, i.e., 10^5 summations in the multichannel analyzer were necessary to get an accuracy of ± 1 kHz in the resonance frequency. The linewidth for both lines was approximately 15–20 kHz. Above room temperature the probe head was kept in a thermostatic bath filled with silicon oil. The temperature was controlled and monitored by two separate platinum resistors. The temperature stability was better than ± 0.01°. Below room temperature the probe head was inserted into a gas-flow cryostat controlled by a platinum resistor.

The measurements were carried out with two crystals originating from different growth runs. Both were grown from solutions saturated at 50 °C by slow cooling. They contained as main imperfections small amounts of mother liquid in the order of 0.1% by weight.[8] Although the crystals were stored in a desiccator containing P_2O_5, they contained enough free water in the bulk to induce line shifts of the ^{35}Cl NQR in the order of 30 kHz. After keeping the crystals for several hours at 400 K they showed reproducible results with identical temperature behavior.

The results are shown in Fig. 2. The first-order phase transition at 256.5 K causes a jump in both NQR frequencies. Within the accuracy of the temperature measurements (± 0.05°) no hysteresis has been observed. The second-order phase transition at 393.7 K gives rise to a critical behavior

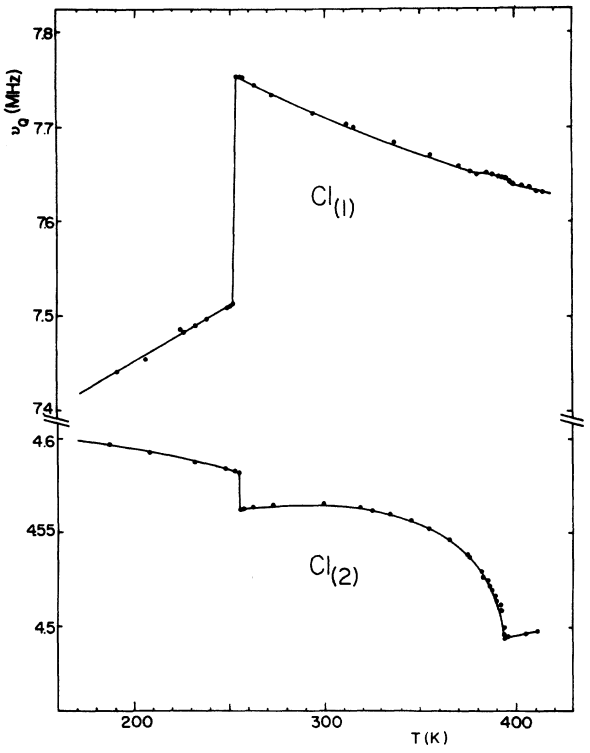

FIG. 2. Temperature dependence of the two ^{35}Cl NQR frequencies in $(CH_3NH_3)_2MnCl_4$.

of the electrical field gradient (efg) at one chlorine site, whereas the efg tensor of the other site is almost unaffected. The critical exponent of $\Delta\nu_{Q(2)}$ was found to be 0.5 from a plot of log $(\Delta\nu_{Q(2)})$ vs $\log(T_c - T)$, where $\Delta\nu_{Q(2)}$ is the difference between the resonance frequency and the extrapolated frequency from the tetragonal phase. In log-log plots, however, the weights of the data points are not taken into account in a correct way and small shifts in T_c may lead to considerable errors in the critical exponents. In Fig. 3, therefore, $\Delta\nu_{Q(2)}$ is plotted vs $(T_c - T)^{1/2}$. In addition the function $y = a(T_c - T + \Delta T)^{\zeta}$ was fitted to $\Delta\nu_{Q(2)}(T_c - T)$ by a least-squares fit for which only data points with $T_c - T < 15\,^{\circ}$K were taken into account. The fitted value of $\Delta T = 0.04\,^{\circ}$K indicates that the measured value of T_c is in good agreement with the fitted value of T_c. The calculated critical exponent ζ is equal to 0.50 ± 0.01.

In order to assign the two resonance frequencies to the corresponding chlorine sites in the lattice, rotation patterns in a small magnetic field of 40 Oe with a rotation axis parallel to the layers of the crystal were measured for the tetragonal phase at 400 K. From the rotation pattern the direction of the principal axes of the electric-field-gradient tensor $\partial^2 V/\partial x_i \partial x_j$ and its asymmetry parameter[9] $\pi \equiv (V_{xx} - V_{yy})/V_{zz}$ may be deduced. The efg tensor belonging to the lower frequency (4.5 MHz) was found to be axially symmetric ($\pi = 0$) with the principal axis z perpendicular to the layers. This allows an unambiguous assignment to the lattice site e of the space group $I4/mmm$ (D_{4h}^{17}) with the point symmetry $4mm$, i.e., the lower-frequency line which shows that the critical behavior belongs to the "nonbonding chlorine" sites above and below the manganese plane ($Cl_{(2)}$). The efg tensor belonging to the higher-frequency line (7.63 MHz) showed a complicated rotation pattern with two sets of extremely weak lines. It did not allow a complete determination of all the efg-tensor elements. All one can say is that an asymmetry parameter π of the order 0.7 exists and that the two efg tensors are connected by a rotation of 90° around the tetragonal axis. This is in agreement with the point symmetry mmm of the lattice site c which is occupied by the "bonding chlorines" in the manganese plane ($Cl_{(1)}$).

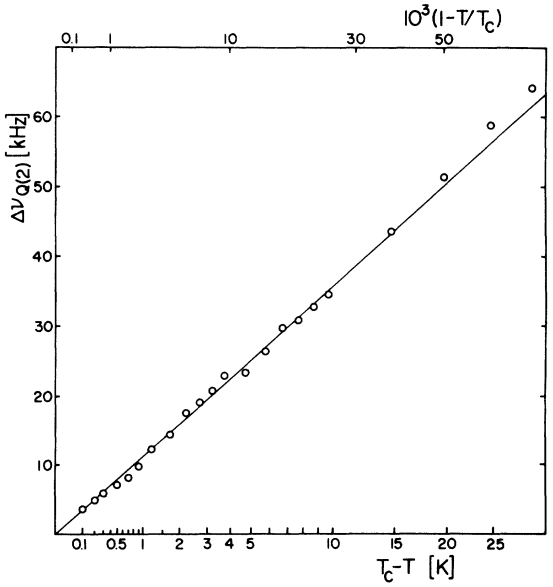

FIG. 3. Frequency shift $\Delta\nu_{Q(2)}$ vs $T_c - T$ on a square-root scale. $\Delta\nu_{Q(2)}$ is the difference between the NQR frequency $\nu_{Q(2)}$ in the orthorhombic phase and the extrapolated one from the tetragonal phase.

III. MICROSCOPIC MODEL AND MECHANISM OF THE PHASE TRANSITION

The question of the dependence of ν_Q on the order parameter η can only be answered if a complete model of the phase transition is constructed which agrees with all experimental data known. Since the space group in the orthorhombic phase is the same as for $(CH_3CH_2CH_2NH_3)_2MnCl_4$ one can adapt the structural data of Ref. 3. The crystal axes we use refer to the space group $Cmca$ (D_{2h}^{18}), where the b axis is perpendicular to the layers and where the mirror plane is perpendicular to the a axis (Fig. 1). According to the literature the orthorhombic phase differs from the tetragonal phase by a shortened a axis, an elongated c axis,[2] and a washboardlike tilting of the $MnCl_6$ octahedra by the angle $\pm\phi$ around the a axes, as well as a frozen-in position of the alkylammonium groups.[3]

The NH_3 protons form hydrogen bonds to the chlorine atoms. The formation of N-H···Cl bonds is proved in two ways: (a) The thermal decomposition of $(CH_3NH_3)_2MnCl_4$ leads to $2(CH_3NH_3Cl) + MnCl_2$.[10] (b) The infrared spectra of aqueous solutions[10] of CH_3NH_3Cl and $(CH_3NH_3)_2MnCl_4$ and of single crystals of the latter substance show two absorption bands at approximately 2400 and 2600 cm^{-1}. These bands must arise from N-H···Cl bonds since if Cl is replaced by OH groups they are absent.[11]

One of the hydrogen bonds is approximately parallel to the c axis and leads to a nonbonding $Cl_{(2)}$ site, whereas the other two lead to bonding $Cl_{(1)}$ in the manganese plane. The three bonds have approximately the same length with bonding angles corresponding to an almost regular tetrahedral arrangement. The N-C bond is, therefore, tilted approximately about 20° with respect

to the b axis. The CH_3NH_3 groups having a trigonal symmetry themselves are certainly rotating around the molecular axis, i.e., for the NH_3 protons a jumpwise rotation between the bonds, and for the CH_3 protons a free rotation. These rotations are expected to freeze in at temperatures well below 200 K as is well known for NH_3 and CH_3 rotations in all such compounds.

In the tetragonal phase an additional rotation of the CH_3NH_3 groups around the fourfold axis must exist in order to fulfill the symmetry conditions. Since the nitrogen position is more or less fixed by the hydrogen bonds, the N-C bonds are moving on a conical surface with a cone angle of 40°. The motion on the cone is not continuous, but a jumpwise rotation for ±90° around the C_4 axis between four equivalent potential wells (Fig. 4).

So far we have considered only structural arguments. Experiments show that the assumed motion exists as described above

(a) The axially symmetric efg tensor ($\pi = 0$) at the nonbonding chlorine sites indicates that the $Cl_{(2)}$ sees a tetragonal charge distribution. There are four possible $Cl_{(2)} \cdots$ H-N bridges to the four neighboring N atoms. At any time one of these bridges will be occupied by a proton, and the probability of occupation must thus be equal for each of the four. This proves the jumpwise rotation

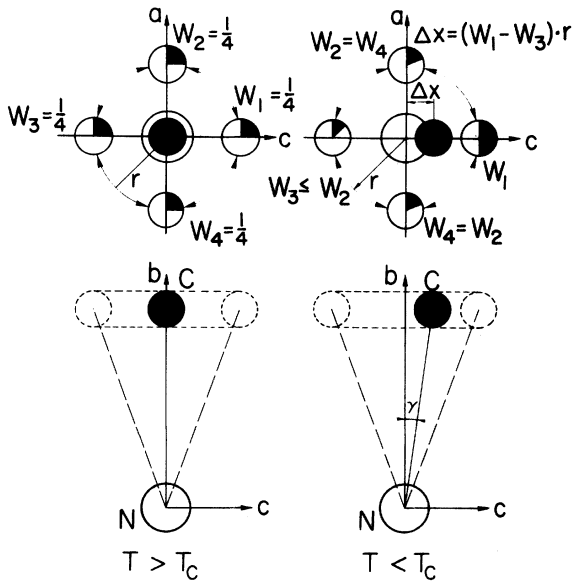

FIG. 4. Motion of the molecular axis N-C of a CH_3NH_3 group above and below T_c in a schematic representation. The probability amplitudes of the four possible carbon positions ($W_1 \cdots W_4$) are indicated by the black areas in the corresponding open circles. The time-averaged position are given by the full circles.

of the NH_3 group around the C_4 axis. The jump rate ω must be much higher than the linewidth, i.e., $\omega > 10^5$ sec^{-1}.

(b) The tilting of the N-C bonds about 20° cannot be proved by these arguments, but if the molecular axes of the CH_3NH_3 groups were parallel to the C_4 axes as it is drawn in Fig. 1 of Ref. 2, the ordering would occur at much lower temperatures ($T_c < 200$ K) for energetic reasons.

(c) Very recent NMR measurements on partially deuterated crystals $(CH_3ND_3)_2MnCl_4$ prove the tilting of the N-C bonds in the tetragonal phase and the four potential wells as well as the fast rotation of the NH_3 and CH_3 groups around the molecular axis.[12]

From the above picture of the tetragonal phase one can try to derive the mechanism of the phase transition. On lowering the temperature, the tumbling motion of the CH_3NH_3 groups becomes more and more coherent because there is an energetically favored number of proton bridges leading to a single Cl site (one bridge for nonbonding $Cl_{(2)}$ sites, two bridges for bonding $Cl_{(1)}$ sites). With increasing coherence length the response amplitude of the $MnCl_4$ matrix especially the amplitude of the soft mode is increased. The group-theoretical analysis of the phase transition[4] $D_{2h}^{17} \rightarrow D_{2h}^{18}$ shows that the soft mode transforms according to a τ_5 representation in the X point of the tetragonal Brillouin-zone boundary, so that the order parameter η has two components η_1 and η_2. The eigenvectors of the soft mode represent a linear combination of the τ_5-symmetry vectors and can be reasonably approximated by a rotation of the $MnCl_6$ octahedra and the CH_3NH_3 groups around the a ($\eta_1 = 0$) or c ($\eta_2 = 0$) axes. η_1 and η_2 are two components of the order parameter, and it is shown[4] that only the simple special cases occur in the orthorhombic phase, where either $\eta_1 = 0$, $\eta_2 \neq 0$, or $\eta_2 = 0$, $\eta_1 \neq 0$. The "rotation" of the CH_3NH_3 groups around the a axis must be seen as a tilting of the time-averaged N-C directions caused by a biasing of the tumbling mode, i.e., one of the four potential wells becomes favored. Figure 4 shows the projection of the motion of one N-C bond on planes perpendicular to the b and a axes for $T > T_c$ and $T < T_c$. For simplification the position of the nitrogen is assumed to be stable. The probability W_1 of finding the carbon atom in the position 1 is illustrated by the black area in the corresponding circle. Above T_c all four positions have equal probabilities, $W_1 = W_2 = W_3 = W_4 = \frac{1}{4}$. The time-averaged carbon position is the center of gravity of the probabilities. Thus the time-averaged direction of the N-C bond coincides with the fourfold axis above T_c. Below T_c the probability W_1 increases with

decreasing temperature and hence the center of gravity moves out of the cone axis by a distance Δx. Since the bc plane is a mirror plane of the orthorhombic phase, W_2 is equal to W_4 and Δx is parallel to the c axis. The deviation Δx is given by

$$\Delta x = (W_1 - W_3) r, \tag{1}$$

where r denotes the radius of carbon-atom motion. For small Δx the tilting angle γ is proportional to Δx.

A definition of the order parameter η_2 could be

$$\eta_2 = (W_1 - \tfrac{1}{4}) f\,, \tag{2}$$

where f is a normalization factor. From the proportionality of Δx and η_2 (see Ref. 4) we get

$$\begin{aligned} W_1 - W_3 &= c(W_1 - \tfrac{1}{4})\,, \\ W_3 &= W_1(1-c) + \tfrac{1}{4}c\,. \end{aligned} \tag{3}$$

The normalization factor f becomes

$$f = 4(c-1)\,, \tag{4}$$

if complete order ($\eta_2 = 1$) for $W_3 = 0$ is assumed. The system has physically significant solutions for $\frac{4}{3} \leq c \leq 2$. The two limiting cases are

$$W_3 = W_2 = W_4 = \tfrac{1}{3}(1 - W_1)$$

and (5)

$$W_3 = \tfrac{1}{2} - W_1, \quad W_2 = W_4 = \tfrac{1}{4}\,.$$

For $c > \frac{4}{3}$ the system reaches with increasing W_1 a state where $W_3 = 0$ and $W_2 = W_4 \neq 0$ if Eq. (3) still holds so far away from the phase transition. Any further increase of W_1 probably results in a new phase transition.

A complete freezing in of the tumbling motion in the favored potential well at the phase transition would cause a flip in the time-averaged N-C directions about 20° and does not agree with a second-order phase transition. The transition entropy of[13] 0.03 cal/mol K is in fact too small for a complete freezing in of the tumbling mode. The NMR-NQR investigations of the deuteron sites in $(CH_3ND_3)_2MnCl_4$ indicate that the tumbling mode exists down to the first-order phase transition at 256 K where γ is approximately 14°.[11] If the same is true for $(CH_3CH_2CH_2NH_3)_2MnCl_4$ the N and C positions of Ref. 3 must be the time average of the tumbling mode.

It follows from the group-theoretical analysis of Ref. 4 that the deformation and the birefringence vary as the square of the order parameter. In contradiction to a statement made in Ref. 2 this is not generally true for order-disorder transitions with a change in crystal symmetry. For the order-disorder transition in KH_2PO_4 a linear dependence of the birefringence on the order parameter was observed[14] and such a behavior must be expected for all cases with nonvanishing piezoelectric constants. The dependence of $\Delta\nu_{Q(i)}$ on the order parameter is thus not trivial and will be evaluated in Sec. IV for the above model of the phase transition.

IV. CALCULATION OF Cl NQR FREQUENCY DEPENDENCE ON THE ORDER PARAMETER

A. Point-charge model

The ^{35}Cl NQR frequency is given by

$$\nu_Q = \frac{e^2 q Q (1-\gamma^\infty)}{2h}\left(1 + \frac{\pi^2}{3}\right)^{1/2}, \tag{6}$$

where eQ is the nuclear quadrupole moment, $eq \equiv \partial^2 V/\partial z^2$ is the largest component of the efg tensor at the site of the nucleus in the principal-axes representation, $\pi \equiv (V_{xx} - V_{yy})/V_{zz}$ is the asymmetry parameter, and γ^∞ is the antishielding factor.[15] The efg tensor is a traceless second rank tensor caused by the charges surrounding the nucleus. The usual attempts at calculating efg tensors start with a point-charge model of the crystal lattice by assuming that the influence of the electrons belonging to the investigated nucleus can be taken into account by an antishielding factor. The second step is then to introduce effective charges and their effective distances to the investigated nucleus in order to fit theory to experimental data. Usually such attempts do not lead to satisfying results, but there are situations where the application of a point-charge model is useful for qualitative arguments as in the case of the phase transition under study. With the simulation of the phase transition in a point-charge model we tried to obtain answers to the following questions: (a) What is the relation between order parameter and $\nu_{Q(2)}$ for the nonbonding $Cl_{(2)}$ sites? (b) Why is $\nu_{Q(1)}$ of the bonding $Cl_{(1)}$ sites not affected by the phase transition?

The simulation was started by constructing the tetragonal phase with the coordinates of the orthorhombic space group $Cmca$, i.e., $a = c$, $\phi = 0$, and $\gamma = 0$. The tumbling mode was simulated by placing positive charges on all possible proton sites. The probability of finding a proton at a given site was expressed by weighting the charges ($+\frac{1}{4}e$ for the bonds to the off-plane $Cl_{(2)}$ sites and $+\frac{1}{2}e$ for the bonds to the inplane $Cl_{(1)}$ sites). Figure 5 shows the situation in a plane parallel to the layers cutting the N and the nonbonding $Cl_{(2)}$ sites.

For the charges of the other atoms the following assumptions were made: CH_3 is neutral, N is $-2e$, H is $+e$, Mn is $+2e$ and Cl is $-e$. Since only

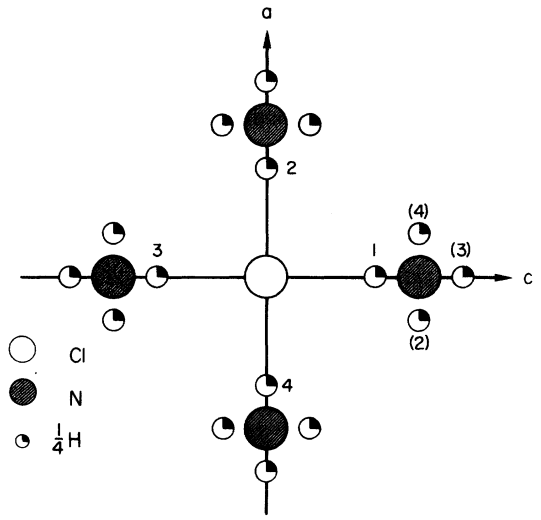

FIG. 5. Positions of the atoms in a plane parallel to the layers cutting the N and the nonbonding $Cl_{(2)}$ sites in the tetragonal phase.

van der Waals forces are acting between the CH_3 groups of adjacent layers their charge can be neglected. Thus a CH_3NH_3 group has the charge $+e$ and the Mn^{++} has the charge $+2e$. The other charges are chosen to give a neutral system.

The lattice sum for the efg tensors of the two Cl sites gives $eq = +0.150$ Å^{-3}, $\pi = 0$ for the off-plane site, and $eq = +0.241$ Å^{-3}, $\pi = 0.85$ for the in-plane site. The ratio of the measured NQR frequencies differs only by 5% from the calculated ratio. This surprisingly good agreement might be an accident but in the case of $(CH_3CH_2NH_3)_2CuCl_4$ we obtained similar results (measured: $\nu_{Q(1)} = 11.507$ MHz, $\nu_{Q(2)} = 11.094$ MHz, $\nu_{Q(1)}/\nu_{Q(2)} = 1.04$, calculated ratio based on the structure determination[16] $\nu_{Q(1)}/\nu_{Q(2)} = 1.24$).

The efg tensors being calculated with respect to the orthorhombic axes are in general not diagonal. Since the poor signal-to-noise ratio of the ^{35}Cl NQR signals did not allow a complete determination of the efg tensors (π and the orientation of the principal axes are not known in the orthorhombic phase), the comparison between theory and experiment is limited to the frequency ν_Q. This has a serious disadvantage because ν_Q does not depend linearly on changes in the elements of the efg tensor.

B. Analytical calculation of the NQR line shift for the $Cl_{(2)}$ site in a two-dimensional model

To get a physical feeling for the relative importance of the various contributions to the line shift we first solve a simplified two-dimensional model shown in Fig. 5. Here only changes in the efg tensor occurring from the neighboring proton are taken into account. In the tetragonal phase above T_c there is a strong positive efg tensor A_{ik} with $\pi = 0$ and $\vec{z} \| \vec{b}$ resulting from the lattice without protons. The influence of the neighboring proton is given by two tensors B_{ik} and C_{ik} with $\pi = 0$, $\vec{z} \| \vec{a}$ and $\vec{z} \| \vec{c}$ which differ only in orientation. The probability of finding the proton in one of the four $Cl_{(2)}$-N directions is given by W_1, W_2, W_3, and W_4 as used for carbon positions in Sec. III. The total efg tensor T_{ik} becomes

$$T_{ik} = A_{ik} + (W_1 + W_3)C_{ik} + (W_2 + W_4)B_{ik} \,. \tag{7}$$

$$T_{ik} = \begin{pmatrix} -a & 0 & 0 \\ 0 & +2a & 0 \\ 0 & 0 & -a \end{pmatrix} + (W_1 + W_3)\begin{pmatrix} -b & 0 & 0 \\ 0 & -b & 0 \\ 0 & 0 & 2b \end{pmatrix} + (W_2 + W_4)\begin{pmatrix} 2b & 0 & 0 \\ 0 & -b & 0 \\ 0 & 0 & -b \end{pmatrix}.$$

so that

$$T_{ik} = \begin{pmatrix} -a + \frac{1}{2}b & 0 & 0 \\ 0 & 2a - b & 0 \\ 0 & 0 & -a + \frac{1}{2}b \end{pmatrix} = \begin{pmatrix} -t & 0 & 0 \\ 0 & 2t & 0 \\ 0 & 0 & -t \end{pmatrix}, \quad \pi = 0, \quad \vec{z} \| \vec{b} \,. \tag{8}$$

By using the order parameter η_2 of Eq. (2) in the limiting case $c = \frac{4}{3}$, the transition from the tetragonal to the orthorhombic phase is obtained

$$W_1 = \tfrac{3}{4}\eta_2 + \tfrac{1}{4}, \tag{9}$$

$$W_1 \neq W_2 = W_3 = W_4 = \tfrac{1}{4}(1 - \eta_2). \tag{10}$$

Equation (7) now reads

$$T'_{ik} = A_{ik} + (\tfrac{1}{2} + \tfrac{1}{2}\eta_2)C_{ik} + (\tfrac{1}{2} - \tfrac{1}{2}\eta_2)B_{ik} \,, \tag{11}$$

so that

$$T'_{ik} = T_{ik} + \tfrac{1}{2}\eta_2 C_{ik} - \tfrac{1}{2}\eta_2 B_{ik} \,, \tag{12}$$

$$T'_{ik} = \begin{pmatrix} -t - \frac{3}{2}\eta_2 b & 0 & 0 \\ 0 & 2t & 0 \\ 0 & 0 & -t + \frac{3}{2}\eta_2 b \end{pmatrix}. \quad (13)$$

The asymmetry parameter π becomes

$$\pi = 3\eta_2 b/2t, \quad (14)$$

whereas $eq = 2t$ remains unchanged as long as the condition $|\frac{3}{2}\eta_2 b| < |t|$ is fulfilled. By putting this result into Eq. (6) we get

$$\nu_{Q(2)} = \frac{e^2 qQ(1-\gamma^\infty)}{2h}\left(1 + \frac{3b^2}{4t^2}\eta_2^2\right)^{1/2}, \quad (15)$$

and with a linear expansion for small π we find a quadratic dependence on the order parameter η_2

$$\Delta\nu_{Q(2)} = \frac{e^2 qQ(1-\gamma^\infty)}{2h}\ \frac{3b^2}{8t^2}\eta_2^2 + \cdots . \quad (16)$$

Equation (16) shows that a complete freezing in of the tumbling mode at the phase transition would cause a jump in $\nu_{Q(2)}$ which was not observed. It can be seen immediately from Eqs. (5) and (7) that the efg tensor T_{ik} and hence also $\nu_{Q(2)}$ are not affected by the ordering of the neighboring protons in the limiting case $c = 2$. As mentioned in Sec. III the ordering is accompanied by a tipping of the $MnCl_6$ octahedra about the angle $\pm\phi$ and by a deformation $\xi = (c-a)/c$ of the lattice. These two effects have an additional influence on $\nu_{Q(2)}$, which has to be taken into account. The calculation based on the two-dimensional model of Fig. 5 is easy to perform. The tipping of the octahedra leads in a first approximation to a displacement ϵ of the $Cl_{(2)}$ into the direction of the proton site 1. Because of the symmetry properties of efg tensors the effect of the deformation can be simply described by a single positive charge at the proton site 2 approaching the $Cl_{(2)}$ site by the distance δ along the a direction. The change in the efg tensor is given for the latter case by

$$\Delta B_{zz} = \frac{1}{(r-\delta)^3} - \frac{1}{r^3} \simeq \left(3\frac{\delta}{r} + 6\frac{\delta^2}{r^2} + 10\frac{\delta^3}{r^3} + \cdots\right) b . \quad (17)$$

By neglecting higher-order terms we get

$$\Delta B_{ik} = \begin{pmatrix} 3\frac{\delta}{r}b & 0 & 0 \\ 0 & -\frac{3\delta}{2r}b & 0 \\ 0 & 0 & -\frac{3\delta}{2r}b \end{pmatrix} \quad (18)$$

and hence

$$T'_{ik} = \begin{pmatrix} -t + \frac{3\delta}{r}b & 0 & 0 \\ 0 & 2t - \frac{3\delta}{2r}b & 0 \\ 0 & 0 & -t - \frac{3\delta}{2r}b \end{pmatrix}. \quad (19)$$

Since $\Delta eq = \frac{3}{2}(b/r)\delta$, $\Delta\nu_{Q(2)}$ is proportional to $-\delta$, i.e., $\Delta\nu_{Q(2)}$ is proportional to $-\eta_2^2$.

For the tipping the change in the efg tensor is given by

$$\Delta C_{zz} = \frac{1}{(r+\epsilon)^3} + \frac{1}{(r-\epsilon)^3} - \frac{2}{r^3} \simeq \left(12\frac{\epsilon^2}{r^2}\right) b . \quad (20)$$

In this case the odd terms in the expansion vanish and $\Delta\nu_{Q(2)}$ becomes proportional to $-\epsilon^2$. Since ϵ is proportional to ϕ and to η_2, $\Delta\nu_{Q(2)}$ is proportional to $-\eta_2^2$.

The deformation and the tilting of the octahedra are almost orthogonal to each other so that coupling terms between them are expected to vary with η_2^4. This is not the case for the tilting and the ordering where a bilinear term $\Delta\nu_{Q(2)}(\phi\eta_2)$ has to be taken into account. If the proton motion is neglected ($\eta_2 = \text{const}$) as in our first approach[17] this term depends only on ϕ and leads to a wrong result.

C. Numerical calculations of the Cl NQR line shifts by simulating the phase transition in a three-dimensional point-charge model

To get an idea of the magnitude of all contributions to $\Delta\nu_{Q(i)}$ the phase transition was computer simulated for the whole lattice by varying the lattice constants and the atom coordinates. The various proton charges were expressed by the corresponding probability amplitudes W_j. The effects on $\nu_{Q(i)}$ were derived from the lattice sums of the point-charge model. This procedure was necessary especially for the $Cl_{(1)}$ site, because this case cannot be treated with a two-dimensional model. The atom coordinates used in the point-charge model were calculated by using the layer configuration and the Mn-Cl distances of Ref. 3 and the lattice constants of Ref. 2.

In order to obtain realistic results the relation between the three parameters ξ, ϕ, and η_2 and the value of c had to be estimated. From the group-theoretical analysis of Ref. 4 we know

$$\xi = k_1^2\eta_2^2, \quad (21)$$

$$\phi = k_2\eta_2, \quad (22)$$

and hence

$$\phi = (k_2/k_1)\,\xi^{1/2}. \tag{23}$$

With the assumption $\eta_2 = 1$ and $W_3 = 0$ at 256 K, k_1 can be obtained using the deformation ξ from Ref. 2 $k_1^2 = 9.1\times10^{-3}$. Since the tilting angle ϕ is known only for $(CH_3CH_2CH_2NH_3)_2MnCl_4$, the ratio $k_2/k_1 = 46.7°$ was taken from there and one gets $k_2 = 4.45°$. The extent of the critical region down to 256 K, where $T_c - T = 138$ °K, is justified by the measurements of Ref. 2. The measured deviations of $\Delta\nu_{Q(2)}(T)$ from the $(T_c - T)^{\zeta}$ law, however, already become significant for $T_c - T > 15$ °K owing to higher-order effects. At $T_c - T = 15$ °K the values of the parameters are $\eta_2 = 0.56$, $\xi = 2.85\times10^{-3}$, and $\phi = 2.49°$. From Fig. 2 one gets $\Delta\nu_{Q(1)} = 0$ and $\Delta\nu_{Q(2)} = 43$ kHz for this temperature. The constant c denoting how the increase in W_1 is shared between W_3 and $W_2 = W_4$ may be estimated by using the fact that the tilting angle γ of the time-averaged N-C direction reaches only 70% of the cone angle for complete order.[12] Introducing this into Eqs. (1) and (3) one obtains $c = 1.55$.

The calculated efg tensors of the point-charge model were diagonalized and the $\nu_{Q(i)}$ were calculated using Eq. (6) with $e^2Q(1-\gamma_\infty)/2h = 1$. The frequency differences $\Delta\nu_{Q(i)}$ were taken between the values of the orthorhombic and those of the tetragonal phase.

$$\Delta\nu_{Q(i)} = \nu_{Q(i)}(\eta_2, \xi, \phi) - \nu_{Q(i)}(0, 0, 0). \tag{24}$$

The computer simulation of the phase transition in the point-charge model yielded the following relation:

$$\begin{aligned}\Delta\nu_{Q(i)} &= u_{(i)}\eta_2^2 + v_{(i)}\xi + w_{(i)}\phi^2 + s_{(i)}\eta_2\phi \\ &= (u_{(i)} + v_{(i)}k_1^2 + w_{(i)}k_2^2 + s_{(i)}k_2)\eta_2^2 = q_{(i)}\eta_2^2, \\ &\qquad\qquad i = 1, 2 \\ &(u_{(1)} = 0,\ v_{(1)} > 0, w_{(1)} < 0,\ s_{(1)} < 0) \\ &(u_{(2)} > 0,\ v_{(2)} < 0, w_{(1)} < 0,\ s_{(2)} < 0)\end{aligned} \tag{25}$$

where $u_{(i)}$, $v_{(i)}$, $w_{(i)}$, $s_{(i)}$, and $q_{(i)}$ denote the coefficients for proton ordering, deformation, tilting, bilinear coupling between proton ordering and tilting, and total contribution, respectively. The dependence of $\Delta\nu_{Q(i)}$ on the parameters were tested up to the limits given by the parameter values at $T_c - T = 15$ °K and the accuracy of Eq. (25) was found to be better than ±0.1% within these limits. Equation (25) also holds for both limiting cases of the constant c ($c = \frac{4}{3}$ and 2).

The critical exponent ζ of $\Delta\nu_{Q(2)}$ determined in Sec. II is therefore twice the critical exponent β of the order parameter.

$$\beta = \tfrac{1}{2}\zeta = 0.250 \pm 0.005. \tag{26}$$

Since $q_{(1)}$ was measured to be zero, we have

$$v_{(1)}k_1^2 + w_{(1)}k_2^2 + s_{(1)}k_2 = 0. \tag{27}$$

We assume that for $Cl_{(1)}$ the various contributions compensate each other by accident. Some evidence for this was obtained from ^{35}Cl NQR measurements for the equivalent phase transition $D_{4h}^{17} - D_{2h}^{18}$ in $(CH_3CH_2NH_3)_2CuCl_4$ where the Mn ions are replaced by Cu ions. Figure 6 shows the temperature dependence of $\nu_{Q(1)}$ and $\nu_{Q(2)}$. Although the phase transition is of first order one can see that $q_{(1)} \neq 0$ for this case.

According to the measurements (Fig. 2) the constant $q_{(2)}$ in $(CH_3NH_3)_2MnCl_4$ is positive. From Eq. (25) we know that only the ordering of the protons $u_{(2)} > 0$ gives a positive contribution to the NQR line shift of the $Cl_{(2)}$ sites. With the two-dimensional model we have shown that the ordering of the neighboring protons increases the asymmetry parameter π of the efg tensor resulting in an increase of $\nu_{Q(2)}$ [see Eqs. (15) and (16)]. The increase of π is significant only if the constant c is smaller than the upper limiting value, i.e., $c < 2$. In the computer simulation a positive value of $q_{(2)}$ was obtained only for $c < 1.57$. This proves that not only the probability amplitude W_3 but also W_2 and W_4 decrease with increasing W_1.

So far the calculated values of $\Delta\nu_{Q(i)}$ were expressed in units of $Å^{-3}$. As soon as one needs $\Delta\nu_{Q(i)}$ in frequency units, in order to compare them with measurements, one has to make assumptions which do not generally hold. In our case we made the assumption that the relative change in the measured resonance frequency is equal to the relative change in the calculated res-

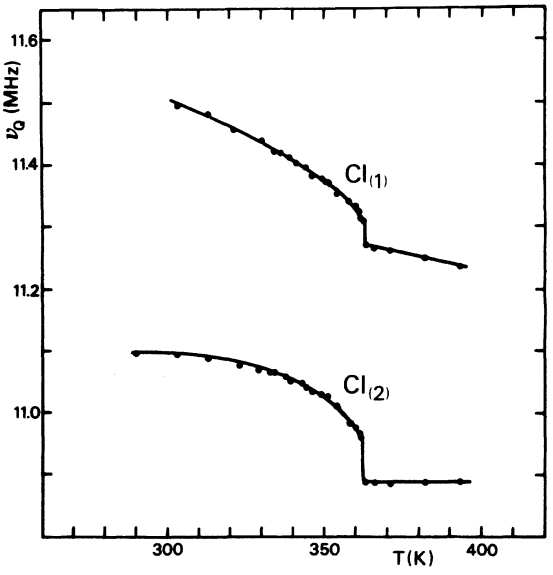

FIG. 6. Temperature dependence of the two ^{35}Cl NQR frequencies in $(CH_3CH_2NH_3)_2CuCl_4$.

TABLE I. Computed values of the various contributions to the shifts in the NQR frequencies according to Eq. (25) in kHz for the parameters $\eta_2 = 0.56$, $\xi = 2.85 \times 10^{-3}$, and $\phi = 2.29°$ determined at $T_c - T = 15$ °K. The results are shown for the two limiting cases of the constant c ($c = 2$, $c = \frac{4}{3}$) as well as for the intermediate value $c = 1.50$, which gives the best fit with the experiment.

c	$u_{(1)}\eta_2^2$	$v_{(1)}\xi$	$w_{(1)}\phi^2$	$s_{(1)}\eta_2\phi$	$q_{(1)}\eta_2^2$	$u_{(2)}\eta_2^2$	$v_{(2)}\xi$	$w_{(2)}\phi^2$	$s_{(2)}\eta_2\phi$	$q_{(2)}\eta_2^2$
2	0	+38	−25	−9	+6	+10	−12	−12	−11	−25
$\frac{4}{3}$	0	+38	−25	−18	−5	+293	−12	−12	−21	+248
1.50	0	+38	−25	−13	0	+83	−12	−12	−16	+43
Measured $\Delta\nu_{Q(i)}$ at $T_c - T = 15$ °K					0					+43

onance frequency:

$$\frac{\Delta\nu_{Q(i)}}{\nu_{Q(i)}}(\text{calc}) = \frac{\Delta\nu_{Q(i)}}{\nu_{Q(i)}}(\text{meas}).$$

This implies that the antishielding factor $1 - \gamma^{\infty}$ of the Cl ion is the same for the whole calculated external efg tensor as well as for small changes in it. This is certainly not true if covalent bonding is present. A fit of the theory to the experiment $[q_{(2)}(\text{calc}) = q_{(2)}(\text{meas})]$ has therefore to be interpreted with some caution. Our point-charge model, however, allows values of $q_{(2)}$ to be fitted within a large range $[0 < q_{(2)} < 6q_{(2)}(\text{meas})$ with $q_{(1)} = 0]$. Since η_2 is given by definition, and since the deformation ξ is measured (i.e., k_1 is known), only k_2 and c were used to fit theory and experimental data. The fit yielded $k_2 = 4.1°$ and $c = 1.50$, a result which agrees very well with the estimated values. Table I gives an idea of the magnitudes of the different contributions to $\Delta\nu_{Q(i)}$ according to Eq. (25).

The success of the point-charge model in the case of $(CH_3NH_3)_2MnCl_4$ is probably due to the following facts. The efg tensor at the origin of a coordinate system caused by a single point charge at the site $\vec{r}$ decreases with r^{-3}. On the other hand, the number of charges in a sphere of a crystal with radius r increases with r^2. Although an r^{-1} dependence of the contributions to the lattice sum results, the lattice sum converges within a few lattice constants because of the neutrality of the system. This was tested for our model by using different ways of summation.[18-20] Therefore, the contribution of next neighbors is dominant, in our case the contributions of the Mn and the protons $r \simeq 2.5$ Å. If one takes a single $Cl_{(2)}$ site with its neighboring Mn atom and proton one gets

$$eq_{\text{Mn,H}}(Cl_{(2)}) = eq_{\text{Mn}} + eq_{\text{H}} = 0.26 - 0.07 = 0.19 \text{ Å}^{-3},$$

whereas the whole lattice sum for all charges yields $eq = 0.15$ Å^{-3}. Similar results are obtained for the $Cl_{(1)}$ site. The main contributions to $\Delta\nu_{Q(i)}$ at the chlorine sites are therefore due to changes in the Cl-Mn and Cl-H distances as well as to the ordering of the protons.

V. CONCLUSIONS

We have constructed a microscopic model for the structural second-order phase transition in the layer structure $(CH_3NH_3)_2MnCl_4$. The experimental results show that the phase transition is governed by the motion of the CH_3NH_3 groups. We have analyzed this motion to be a jumpwise rotation of the molecular axis on a conical surface connected with the four distinguishable orientations of the NH_3 groups. These orientations are due to the formation of N-H$\cdots$Cl bonds which are responsible for the four potential wells of the jumpwise rotation. In the tetragonal phase the probability amplitudes of the different orientations are equal in time. Below the phase transition the motion of the CH_3NH_3 group becomes biased, i.e., one of the orientations becomes energetically favored. In a system with four potential wells it is not possible without additional information to predict how the probability amplitudes of the less favored orientations will decrease. For symmetry reasons it was possible to describe this decrease with a single constant c. Together with the order parameter η and the related lattice deformation the constant c determines the mechanism of the phase transition.

In order to explain the temperature dependence of the two ^{35}Cl NQR lines the phase transition was computer simulated in a point-charge model based on the microscopic model described above. The calculated shift of the resonance frequencies $\Delta\nu_{Q(i)}$ was found to vary exactly with the square of the order parameter η. The critical exponent β of the order parameter η $[\eta \propto (T_c - T)^{\beta}]$ was found to be somewhat lower ($\beta = 0.25$) than in Ref. 2 ($\beta = 0.315$). The theoretical value of β for a three-dimensional Ising model (cubic fcc, bcc)

is $\beta = 0.312$, whereas for the two-dimensional Ising model a much lower value is calculated ($\beta = 0.125$).[21] Although no theoretical value of β for an orthorhombic three-dimensional Ising model has been calculated up to now, one can say that the coupling between adjacent layers should not be neglected in a theoretical treatment of the phase transition, and thus the layer structures cannot be considered as two-dimensional perovskites.

The computer simulation of the phase transition in the point-charge model allowed not only the temperature dependence of $\Delta\nu_{Q(t)}$ to be explained but also gave a self-consistent proof of our microscopic model.

Recently, Heger[22] has finished detailed structure analyses of the orthorhombic and the tetragonal high-temperature phases of $(CH_3NH_3)_2MnCl_4$. In the tetragonal phase each of the four potential wells is split into two close minima owing to the fact that the N-H$\cdots$Cl bonds are not perfectly straight. This additional splitting is absent in the orthorhombic phase. In reality the motion of the N atoms is also larger than assumed in this paper. Accordingly the C-N motion corresponds to a double cone with the summit between C and N. The proposed mechanism of the phase transition is, however, not altered by these structural adjustments.

ACKNOWLEDGMENTS

We would like to thank Professor R. Blinc for helpful discussions and the critical reading of the manuscript, H. Arend and W. Huber for the crystal growth and for providing unpublished results.

---

†Work supported in part by the Swiss National Science Foundation.

[1]H. Arend, R. Hofmann, and F. Waldner, Solid State Commun. 13, 1629 (1973).
[2]K. Knorr, I. R. Jahn, and G. Heger, Solid State Commun. 15, 231 (1974).
[3]E. R. Peterson and R. D. Willet, J. Chem. Phys. 56, 1879 (1972).
[4]J. Petzelt, J. Phys. Chem. Solids 36, 1005 (1975).
[5]R. Hofmann and H. Arend (unpublished results).
[6]N. J. Tovborg-Jensen, J. Chem. Phys. 50, 559 (1969).
[7]R. Kind and J. Roos, in *Proceedings of the 18th Ampere Congress*, edited by P. S. Allen, E. R. Andrew, and C. A. Bates (University of Nottingham, Nottingham, 1974), p. 297.
[8]H. Arend and W. Huber (unpublished results).
[9]In order to avoid confusion with the order parameter η, the symbol π is used for the asymmetry parameter of the efg.
[10]M. J. Tello, E. H. Bocanegra, M. A. Arrandiaga, and H. Arend, Thermochim. Acta 11, 96 (1975).
[11]J. Petzelt (private communication).
[12]D. Brinkmann, U. Walther, and H. Arend (unpublished).
[13]E. H. Bocanegra, M. J. Tello, M. A. Arrandiaga, and H. Arend, Solid State Commun. (to be published).
[14]B. Zwicker and P. Scherrer, Helv. Phys. Acta 17, 346 (1944).
[15]See, e.g., A. Abragam, *The Principles of Nuclear Magnetism* (Clarendon, Oxford, 1961), Chap. VII.
[16]J. P. Steadman and R. D. Willet, Inorg. Chim. Acta 4, 367 (1970).
[17]R. Kind, J. Roos, and H. Arend, Helv. Phys. Acta 47, 390 (1974).
[18]R. Behrson, J. Chem. Phys. 29, 326 (1958).
[19]C. K. Coogan, Aust. J. Chem. 17, 1 (1964).
[20]F. W. de Wette and G. E. Schacher, Phys. Rev. 137, A78 (1965).
[21]M. E. Fischer, Rep. Prog. Phys. 30, 615 (1967).
[22]G. Heger (private communication).

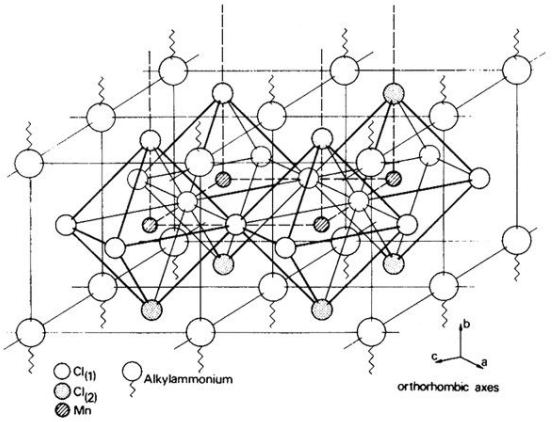

FIG. 1. Schematic representation of perovskite-type layer in $(C_nH_{2n+1}NH_3)_2MnCl_4$.